Anti-inflammatory Potential of Macamides Isolated from Yellow Tubers of Mashua (*Tropaeolum Tuberosum*)

Authors
Luis Apaza Ticona[1, 2]ⓘ, María Rodríguez Coballes[1], Giulia Potente[3], Ángel Rumbero Sánchez[1]

Affiliations
1 Department of Organic Chemistry, Faculty of Sciences, University Autónoma of Madrid, Madrid, Spain
2 Department of Pharmacology, Pharmacognosy and Botany, Faculty of Pharmacy, University Complutense of Madrid, Madrid, Spain
3 Department for Life Quality Studies, University of Bologna, Rimini, Italy

Correspondence
Prof Dr Luis Apaza T
Department of Organic Chemistry, Faculty of Sciences, University Autónoma of Madrid, Cantoblanco
28049 Madrid
Spain
Tel.: + 3491 497 7622 Fax: + 3491 497 4715
luis.apaza@uam.es; lnapaza@ucm.es

ABSTRACT

Although *Tropaeolum tuberosum* tubers have been consumed cooked as a folk remedy for the treatment of skin, lungs, liver and kidneys diseases, these uses have very limited scientific basis. Therefore, this article develops a phytochemical analysis of the yellow tubers of *T. tuberosum* with the objective to assess whether the isolated compounds have anti-inflammatory potential in the CCD-1109Sk, MRC-5 and RWPE-1 cell lines. We performed an extraction of *T. tuberosum* tubers using different organic solvents, followed by a bioguided chromatographic separation. Four macamides were identified by LC/MS techniques, but only *N*-benzyllinoleamide (**1**) and *N*-benzyloleamide (**2**) were isolated and elucidated by NMR/MS techniques, given that they were present in a larger proportion in the tubers. The anti-inflammatory potential of macamides was evaluated by the inhibition of NF-κB and STAT3 activation. Both compounds displayed inhibition of NF-κB activation with IC_{50} values of $2.28 \pm 0.54\,\mu M$; $3.66 \pm 0.34\,\mu M$ and $4.48 \pm 0.29\,\mu M$ for compound (**1**) and $6.50 \pm 0.75\,\mu M$; $7.74 \pm 0.19\,\mu M$ and $8.37 \pm 0.09\,\mu M$ for compound (**2**) in CCD-1109Sk, MRC-5 and RWPE-1 cell lines, respectively. Moreover, both compounds inhibited the STAT3 activation with IC_{50} of $0.61 \pm 0.76\,\mu M$; $1.24 \pm 0.05\,\mu M$ and $2.10 \pm 0.12\,\mu M$ for compound (**1**) and $5.49 \pm 0.31\,\mu M$; $7.73 \pm 0.94\,\mu M$ and $7.79 \pm 0.30\,\mu M$ for compound (**2**). Therefore, isolated macamides of *T. tuberosum* tubers showed promising anti-inflammatory effects, suggesting a possible beneficial use to combat inflammatory processes of skin, lung and prostate.

AG 490	(*E*)-2-Cyano-3-(3,4-dihydrophenyl)-*N*-(phenylmethyl)-2-propenamide
AP-1	Activator protein 1
ATCC	American Type Culture Collection
CB1	Cannabinoid receptor type 1
CRM1	Chromosomal Maintenance 1
DBD	DNA-binding domain
DMEM	Dulbecco's Modified Eagle Medium
DTT	Dithiothreitol
FAAH	Fatty acid amide hydrolase
FAMEs	Fatty acid methyl esters
FBS	Fetal bovine serum
HR-ESIMS	High resolution-Electrospray ionisation mass spectrometry
IFN-γ	Interferon gamma
IκBα	Nuclear factor of kappa light polypeptide gene enhancer in B-cells inhibitor, alpha
IKK	IκB kinase
IL-1β	Interleukin-1 beta
IL-6	Interleukin-6
IL-17	Interleukin-17
L-SIMS	Liquid secondary ion mass spectrometry
JAK	Janus kinase
LDH	Lactate dehydrogenase
MAPK	Mitogen-activated protein kinase
MRM	Multiple reaction monitoring
NF-κB	Nuclear factor kappa B
PBS	Phosphate-buffered saline
PMS	Phenazine methosulfate
PUFAs	Polyunsaturated fatty acids
RLU	Relative light units
SH2	Src Homology 2
STAT3	Signal transducer and activator of transcription 3
TNF-α	Tumour necrosis factor alpha
XTT	2,3-Bis-(2-methoxy-4-nitro5-sulfophenyl)-2H-tetrazolium-5-carboxanilide salt

Introduction

Inflammation has long been a well-known symptom of many infectious diseases, but molecular and epidemiological research increasingly suggests that it is also intimately linked with a broad range of non-infectious diseases [1]. The major steps in an inflammatory cascade are the initiation of the reaction, the progression and the termination, followed by the resolution of inflammation [2]. Infection and inflammation stimulate immune cells to produce a variety of immune mediators including pro-inflammatory cytokines such as: IL-1β, IL-6, TNF-α, NF-κB, STAT3, IFN-γ that are crucial in the inflammation process [3].

In the case of NF-κB, this is a dimeric transcription factor of p50 and p65 subunits, crucial regulator of many physiological and pathophysiological processes, including the control of inflammatory responses [4]. NF-κB relays signals from activated receptors in the plasma membrane to the nucleus, where it regulates gene expression. Canonical NF-κB activation by TNF-α involves phosphorylation and proteasomal elimination of IκBα, uncovering a nuclear localisation signal of NF-κB. Consequently, NF-κB accumulates in the nucleus and regulates the expression of target genes [5].

On the other hand, there are cytokines that express themselves ubiquitously and have more pleiotropic functions, such as STAT3 [6]. Like other members of the STAT family (STAT1, STAT2, STAT4, STAT5A, STAT5B and STAT6), STAT3 signalling involves tyrosine phosphorylation by JAK or other tyrosine kinases, or the nuclear dimerization/translocation [7]. Moreover, in the nucleus, STAT3 binds to DNA and regulates the expression of the target gene. After dephosphorylation, STAT3 dissociates from DNA and leaves the nucleus through CRM1-mediated export to the cytoplasm, where it becomes available for reactivation. Aberrant STAT3 signalling has proven to be a key factor in chronic inflammation and autoimmune conditions, defining STAT3 as a promising therapeutic target [8].

Finally, we must indicate that the NF-κB and STAT3 transcription factors are ubiquitously expressed and control numerous physiological processes including the development, differentiation and immunity of the cell. Both NF-κB and STAT3 are rapidly activated in response to various stimuli including stresses and cytokines, although they are regulated by entirely different signalling mechanisms [9]. The activation of and interaction between STAT3 and NF-κB play a key role in controlling the dialogue between the inflammatory cell and its microenvironment [10].

Currently, synthetic medications such as nonsteroidal anti-inflammatory drugs and biological agents decrease acute and chronic inflammation. However, the use of such agents can cause adverse effects [11]. For this reason, alternatives such as herbal therapies may have a better risk-benefit ratio. In addition, it should be noted that the plants have several chemical components of medicinal importance that can be directed to multiple signalling pathways. It is in this context that the use of medicinal herbs is growing due to their low cost, easy availability and insignificant side effects [12].

Mashua (*Tropaeolum tuberosum* Ruíz & Pavón) is an herbaceous climbing plant that belongs to the Tropaeolaceae family. It grows at altitudes between 3000 and 4000 meters in the cold temperate zones of the Andes. It produces small edible tubers of different colours, the yellow colour being the most consumed because of its anti-inflammatory properties [13]. Documentation has been found that indicates that the cultivation of this plant dates back to the pre-Inca period and currently represents a source of livelihood for the Andean populations [14].

Mashua tubers have been attributed different properties, due to their traditional use, for example their consumption is recommended in the treatment of different skin diseases [13, 15]; lung diseases [13, 16]; urinary diseases [13, 17]; infectious diseases [13, 18] and as an analgesic against kidney and bladder pain [13, 16]. To date, a large number of secondary metabolites present in *T. tuberosum* tubers have been identified and quantified, such as phenolic acids and tannins [19, 20], flavonoids (flavonols and anthocyanins) [19, 21], glucosinolates and isothiocyanates [22], fatty acids [23] and alkamides [24]. Some of these metabolites have been studied to determine if they are responsible for the medicinal properties that are attributed to these tubers.

Apaza et al. Anti-inflammatory Potential of Macamides … Planta Med Int Open 2020; 7: e88–e99

e89

The objective of our work is to determine the anti-inflammatory activity (inhibition of NF-κB and STAT3 activation) of the yellow tubers of *T. tuberosum*. For this analysis we have used different cell lines, taking into account the diseases against which tubers of Mashua have been used in traditional medicine. CCD-1109Sk (skin cells), MRC-5 (lung cells) and RWPE-1 (prostate cells), and a control cell line (THP-1) cell lines were used.

Results and Discussion

CCD-1109Sk (Human skin fibroblast, CRL-2361), MRC-5 (Human lung fibroblast, CCL-171) and RWPE-1 (Human prostate epithelial, CRL-11609) cell lines were selected to carry out the *in vitro* cytotoxicity/viability and activity assays of the *T. tuberosum* extracts and compounds. We have selected these cell lines according to their physiological relationship with certain diseases that are treated in traditional medicine through the consumption of cooked *T. tuberosum* tubers [13]. Therefore, the relationship is: the MRC-5 cell line for lung diseases such as influenza and tuberculosis [13, 16, 25], the RWPE-1 cell line for kidney diseases such as prostatitis and stones in the bladder [13, 26, 27]. In the case of skin diseases such as eczema, ulcers, the CCD-1109Sk cell line was applied in the form of a compress [13, 28, 29]. Furthermore, a cell line (THP-1) was used to assess the safety of the compounds.

Through the LDH and XTT assays (▶ **Table 1**), we observed that the aqueous and *n*-heptane extracts of the yellow tubers of *T. tuberosum* did not show cytotoxicity (LDH) compared to the control (Triton X-100), in addition to being viable (XTT) in the CCD-1109Sk, MRC-5 and RWPE-1 cell lines compared to the control (Actinomycin D). Likewise, we observed that the CH$_2$Cl$_2$/MeOH extract showed cytotoxicity (LDH) in all the cell lines we analysed, in addition to not showing viability (XTT), being discarded from the next research phase of anti-inflammatory activity assays.

To understand the results of the LDH and XTT assays, we must reflect on the action of the extracts at a specific site within the cells. There are two ways in which a cell suffers death, either by exposure to a harmful environment and/or injury (necrosis) or by a process of decomposition (apoptosis) previously planned and regulated. In our case, the LDH assay was used to measure cell necrosis [30] and the XTT assay to determine cell apoptosis [31]. Analysing the results obtained, we can indicate that the aqueous and *n*-heptane extracts did not show cytotoxicity and proved to be viable for the cell lines tested using the LDH and XTT assays, respectively. Finally, no significant differences were observed between both extracts.

With respect to anti-inflammatory activity, only the *n*-heptane extract of the yellow tubers of *T. tuberosum* showed an inhibition of NF-κB and STAT3 in all cell lines. In the case of inhibition of TNF-α-induced NF-κB activation, the *n*-heptane extract showed an IC$_{50}$ of $63.00 \pm 0.03\,\mu g/mL$; $66.03 \pm 0.72\,\mu g/mL$ and $71.76 \pm 0.39\,\mu g/mL$ on CCD-1109Sk, MRC-5 and RWPE-1 cells, respectively (▶ **Table 2**).

Likewise, in the case of inhibition of STAT3 activation induced by IFN-γ, only the *n*-heptane extract of *T. tuberosum* showed activity on the CCD-1109Sk, MRC-5 and RWPE-1 cell lines with an IC$_{50}$ of $55.05 \pm 0.68\,\mu g/mL$; $58.48 \pm 0.38\,\mu g/mL$ and $63.42 \pm 0.51\,\mu g/mL$, respectively (▶ **Table 3**).

Observing the ^{1}H-NMR spectrum of the *n*-heptane extract (▶ **Fig. 1S**), a signal at 7.34 ppm characteristic of the benzyl aromatic protons could be seen. Likewise, characteristic signals of fatty acids mixtures were observed, which were compared with the data reported [32]. These are included in ▶ **Table 1S**, in which the chemical shifts of the *n*-heptane extract were observed. A brief indication is also made to the type of corresponding hydrogens for each group of signals in the spectrum.

Based on the results obtained, the *n*-heptane extract was fractionated by a chromatographic column to isolate its active compounds. From the nine resulting fractions, fraction III was the most active (▶ **Tables 4S-5S**) in all cell lines. For this reason, the respective FAMEs of fraction III (▶ **Fig. 1**) were prepared for further analysis by GC/MS. The results of the GC/MS determination of the FAMEs present in fraction III (▶ **Fig. 1**) showed that the main fatty acids were: palmitic, oleic and linoleic (▶ **Table 4**).

The results obtained corroborate the results found in the literature, which mention that the main fatty acids present in *T. tuberosum* are: palmitic (C16:0), linoleic (C18:2) and α-linolenic (C18:3) [23]. In our work, we have identified a total of nine fatty acids in fraction III, while previous authors have reported the presence of

▶ **Table 1** LDH and XTT assays of the extracts from *T. tuberosum* against a panel of human cell lines after 12 h of treatment.

Samples	% Viable cells			
	THP-1	CCD-1109Sk	MRC-5	RWPE-1
Untreated cells	99.96 ± 0.27	96.95 ± 0.50	97.11 ± 0.01	97.85 ± 0.39
Triton X-100	10.61 ± 0.93	11.45 ± 0.94	9.38 ± 0.57	10.71 ± 0.92
n-Heptane extract[a]	96.78 ± 0.42	92.79 ± 0.51	93.81 ± 0.87	93.93 ± 0.27
CH$_2$Cl$_2$/MeOH extract[a]	60.62 ± 0.41	62.05 ± 1.63	67.42 ± 0.47	68.07 ± 1.76
Aqueous extract[a]	$> 100 \pm 1.16$	97.76 ± 0.82	97.15 ± 0.53	98.60 ± 2.09
Untreated cells	100.01 ± 0.28	98.96 ± 0.31	99.90 ± 0.32	99.99 ± 1.94
Actinomycin D	50.54 ± 0.56	49.73 ± 0.58	50.59 ± 0.44	47.79 ± 0.55
n-Heptane extract[b]	98.32 ± 0.36	94.00 ± 0.89	94.19 ± 0.02	94.30 ± 1.26
CH$_2$Cl$_2$/MeOH extract[b]	61.02 ± 0.45	66.33 ± 0.43	68.21 ± 0.10	68.64 ± 0.04
Aqueous extract[b]	$> 100 \pm 1.37$	98.20 ± 0.64	97.44 ± 0.21	98.73 ± 2.34

[a]Cytotoxicity values of the LDH assay. [b]Viability values of the XTT assay. The results are the means (± SD) of three separate experiments performed in triplicate. Control = untreated cells. Significant difference among means (p < 0.0001)/Tukey's multiple comparisons test.

▶ **Table 2** Effect of the extracts from *T. tuberosum* on TNF-α-induced NF-κB activation.

Samples	IC$_{50}$			
	THP-1	CCD-1109Sk	MRC-5	RWPE-1
TNF-α 30 *ng*/mL	> 100 ± 0.35	97.72 ± 0.14	99.87 ± 0.12	99.93 ± 0.07
Celastrol (7.41 *μ*M) + TNF-α 30 *ng*/mL	49.48 ± 0.07	47.75 ± 0.75	53.56 ± 0.06	55.59 ± 0.57
n-Heptane extract (*μ*g/mL) + TNF-α 30 *ng*/mL	72.45 ± 0.72	63.00 ± 0.03	66.03 ± 0.72	71.76 ± 0.39
Aqueous extract (*μ*g/mL) + TNF-α 30 *ng*/mL	97.90 ± 0.91	90.80 ± 0.45	92.84 ± 0.90	95.32 ± 0.21
Results are represented as the percentage of inhibition considering 100 % of the value of TNF-α-induced NF-κB activation and are the means (± SD) of three separate experiments performed in triplicate. Control = untreated cells. Significant difference among means (p < 0.0001)/Tukey's multiple comparisons test.				

▶ **Table 3** Extracts of *T. tuberosum* inhibit IFN-γ-induced STAT3 activation.

Samples	IC$_{50}$			
	THP-1	CCD-1109Sk	MRC-5	RWPE-1
IFN-γ 25 U/mL	99.98 ± 0.53	97.20 ± 0.67	98.23 ± 0.93	99.00 ± 0.68
AG 490 (48 *μ*M) + IFN-γ 25 U/mL	51.20 ± 0.57	46.20 ± 0.73	47.70 ± 0.31	48.81 ± 0.43
n-Heptane extract (*μ*g/mL) + IFN-γ 25 U/mL	60.54 ± 0.11	55.05 ± 0.68	58.48 ± 0.38	63.42 ± 0.51
Aqueous extract (*μ*g/mL) + IFN-γ 25 U/mL	96.45 ± 0.31	85.20 ± 0.34	88.12 ± 0.79	90.16 ± 0.85
Results are represented as the percentage of inhibition considering 100 % of the value of IFN-γ-induced STAT3 activation and are the means (± SD) of three separate experiments performed in triplicate. Control = untreated cells. Significant difference among means (p < 0.0001)/Tukey's multiple comparisons test.				

fourteen fatty acids [23]. This difference is due to the fact that in these previous works authors used dehydrated tubers flour (six different varieties), and the esterification was made from an extract enriched in fat without additional fractionation.

Analysing the six subfractions obtained from fraction III using a chromatographic column, we observed that the sub-fraction IIID showed the highest activity (▶ **Tables 6S**-**7S**) in all cell lines, proceeding to analyse the sub-fraction IIID by LC/MS. ▶ **Fig. 2** shows the LC/MS chromatogram resulting from the identification of four macamides present in the sub-fraction IIID.

To identify which macamide corresponds to each MS spectrum, the fatty acids present in fraction III (myristic, palmitic, palmitoleic, sapienic, stearic, oleic, vaccenic, linoleic and α-linolenic) were first analysed (▶ **Fig. 8S**). Subsequently, knowing the molar masses of these fatty acids, and that the macamides are formed through the reaction between the hydroxyl group of the fatty acid and the amino group of the benzylamine [33], we managed to determine the molar masses of the different macamides (▶ **Table 2S**). ▶ **Table 5** shows the retention times, the *m/z* values of the peaks with greater abundance (▶ **Fig. 2**), as well as the ion corresponding to each of the macamides present in the sub-fraction IIID (▶ **Figs. 4S-7S**).

Through the LC/MS technique, we concluded that sub-fraction IIID is composed of the following macamides: *N*-benzylmyristamide, *N*-benzylpalmitamide, *N*-benzyloleamide and *N*-benzyllinoleamide. We also observed the *N*-benzyloleamide and *N*-benzyllinoleamide macamides are found in greater proportion.

Finally, the fractionation of the sub-fraction IIID by means of a chromatographic column led to the obtaining of 14 sub-fractions, where the IIID2 and IIID4 sub-fractions showed greater activity (▶ **Tables 8S**-**9S**). Analysing the IIID2 and IIID4 sub-fractions using ^{1}H-^{13}C-NMR and HR-ESIMS techniques, it was established that these sub-fractions corresponded to the *N*-benzyllinoleamide (**1**) and *N*-benzyloleamide (**2**) macamides (▶ **Fig. 3**).

To date, macamides were thought to be characteristic marker compounds of Maca hypocotyls (*Lepidium meyenii* Walp.) [13]. The presence of eighteen macamides have been reported in Maca, among which *N*-benzylpalmitamide is the most abundant compound in the Maca of Peruvian origin, while *N*-benzyllinoleamide is the richest compound in the Maca of Chinese origin (Yunnan) and is the second most abundant compound in the Peruvian Maca [34]. However, the presence of *N*-oleoyldopamine was recently reported in purple tubers from Mashua (*T. tuberosum*) of Bolivian origin [24]. In our work we confirm that the yellow tubers from Mashua of Bolivian origin are rich in the *N*-benzyloleamide and *N*-benzyllinoleamide macamides; and to a lesser extent in the *N*-benzylmyristamide and *N*-benzylpalmitamide macamides. We can conclude that these types of compounds may be markers of plant species that grow exposed to extreme climatic conditions (poor soils with a slightly acidic pH between 5–6 and exposure to ultraviolet radiation at altitudes of 3.800 meters above sea level), consequently producing this type of compounds. The importance of isolating this type of compounds is due to their chemical nature, since they can easily cross the intestinal wall and the blood-brain barrier, exerting a greater pharmacological effect [13, 34].

Macamides consist of a residue of a benzylamine (product of the hydrolysis of glucosinolates by the enzyme myrosinase, [35]) and a fatty acid residue (product of the hydrolysis of membrane lipids) that gives it a lipophilic property, a physicochemical parameter that determines the ability of a compound to cross the biological membrane [36]. Therefore, macamides that have a long aliphatic chain can easily cross the cell membrane of cells through diffusion, reaching also the mitochondrial membrane.

Apaza et al. Anti-inflammatory Potential of Macamides… Planta Med Int Open 2020; 7: e88–e99

e91

Print Date: 23 May 2017 18:01:02
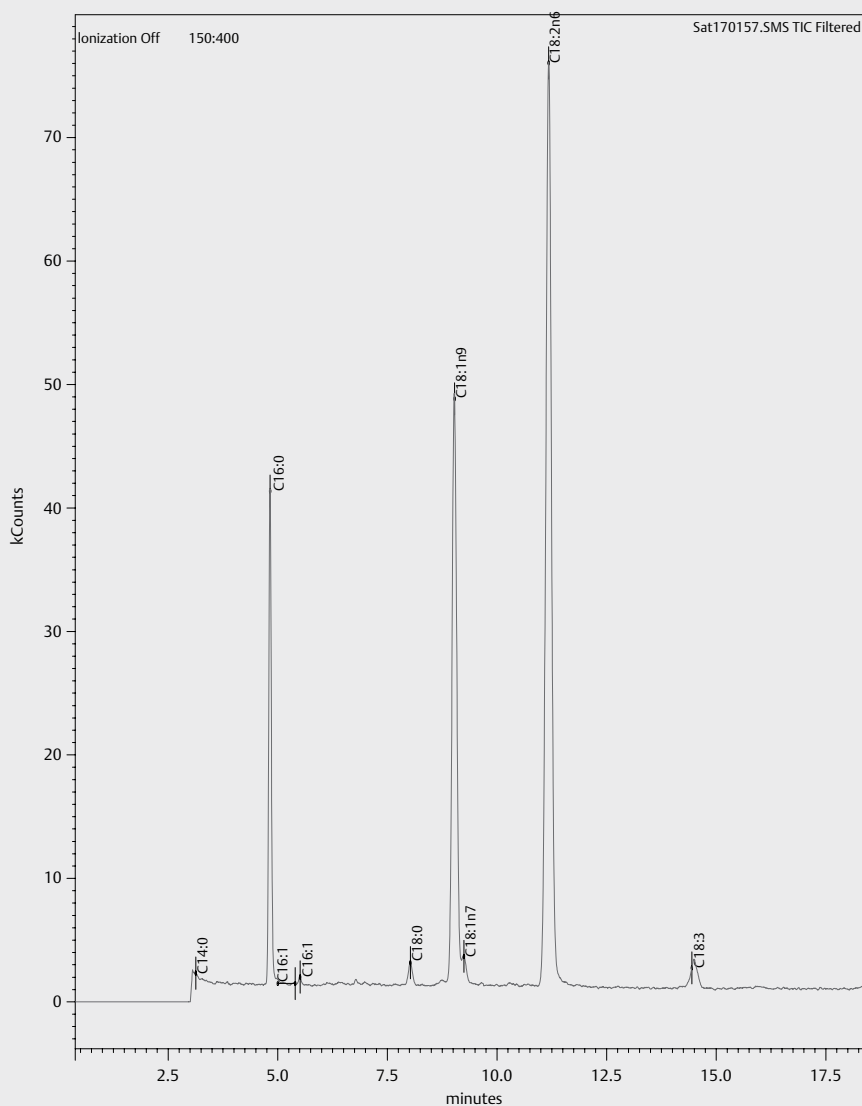
MS Data Review Active Chromatogram Plot - 23/05/2017 18:00

File: c:\varianws\data\muestras 2017\mayo\sat170157.sms
Sample: Sat170157   Operator:
Scan Range: 1 - 11684 Time Range: 0.00 - 66.99 min.   Date: 19/05/2017 14:00

▶ **Fig. 1** GC chromatogram of methyl ester of fraction III of *n*-heptane extract from *T. tuberosum*.

After the isolation and characterisation of the two macamides present in the *n*-heptane extract from the yellow tubers of *T. tuberosum*, cytotoxicity and viability assays were carried out, comparing them with the Triton X-100 and Actinomycin D controls, respectively.

Compound (**1**) *N*-benzyllinoleamide did not show a cytotoxic effect by the LDH assay in CCD-1109Sk, MRC-5 and RWPE-1 cell lines with CC_{50} values of $80.59 \pm 0.90\,\mu$M; $81.42 \pm 0.12\,\mu$M and $82.79 \pm 0.99\,\mu$M, respectively (▶**Table 6**). As regard to the control cell line (THP-1), the CC_{50} was $87.00 \pm 0.07\,\mu$M. Regarding the XTT assay, compound (**1**) had CC_{50} values of $83.09 \pm 0.53\,\mu$M; $85.09 \pm 0.94\,\mu$M and $89.16 \pm 0.57\,\mu$M, respectively (▶**Table 6**), and $89.96 \pm 0.27\,\mu$M in the control cell line (THP-1).

Regarding compound (**2**), *N*-benzyloleamide showed a cytotoxic effect by means of the LDH assay in the CCD-1109Sk, MRC-5 and RWPE-1 cell lines with CC_{50} values of $90.62 \pm 0.85\,\mu$M; $94.51 \pm 0.07\,\mu$M and $95.33 \pm 0.97\,\mu$M, respectively (▶**Table 6**). Concerning the control cell line (THP-1), the CC_{50} was $90.67 \pm 0.58\,\mu$M. Regarding the results of the XTT assay, the compound (**2**) had CC_{50} values of $94.38 \pm 0.11\,\mu$M; $98.45 \pm 0.62\,\mu$M and $99.97 \pm 0.39\,\mu$M, respectively (▶**Table 6**). It had a CC_{50} of $92.45 \pm 0.49\,\mu$M in the control cell line (THP-1).

e92

Apaza et al. Anti-inflammatory Potential of Macamides … Planta Med Int Open 2020; 7: e88–e99

To verify the safety of the compounds, the LDH and XTT assays were chosen, which determine the cytotoxicity/viability at different sites of action. More concretely, with the LDH assay we were able to verify the ability of the compounds to penetrate the cell membrane, and with the XTT assay we could verify the ability of the compounds to act at the level of the mitochondrial membrane [37]. Analysing the results obtained from both the cytotoxicity and viability assays (LDH and XTT), we observe that the data for the two compounds are similar to each other and there are no significant differences.

On the contrary, when comparing the results obtained between the compounds, it is evident that compound (**1**) has a slight cytotoxicity (LDH) and a lower decrease in viability (XTT) with respect to the compound (**2**) and this difference can be justified by account-

▶ **Table 4** Methyl esters of fatty acids present in fraction III of the *n*-heptane extract from *T. tuberosum*.

| Peak	Retention time (min)	Peak area	Designation	Fatty acid
1	3.137	619	C14:0	Myristic
2	4.828	128 610	C16:0	Palmitic
3	5.398	290	C16:1	Palmitoleic
4	5.512	1475	C16:1	Sapienic
5	8.028	9238	C18:0	Stearic
6	9.033	18 875	C18:1n9	Oleic
7	9.252	3380	C18:1n7	Vaccenic
8	11.184	168 056	C18:2n6	Linoleic
9	14.444	3062	C18:3	α-Linolenic

▶ **Table 5** Retention times with *m/z* of the peaks and the most abundant ions of the macamides present in the subfraction IIID of *T. tuberosum*.

| Retention time (min)	*m/z* Peak of greater abundance	Ion	Corresponding macamide
17.3	368.4	$C_{25}H_{38}NO^+$	N-benzyllinoleamide
19.6	318.4	$C_{21}H_{36}NO^+$	*N*-benzylmyristamide
20.5	344.3	$C_{23}H_{38}NO^-$	*N*-benzylpalmitamide
21.7	370.4	$C_{25}H_{40}NO^-$	*N*-benzyloleamide
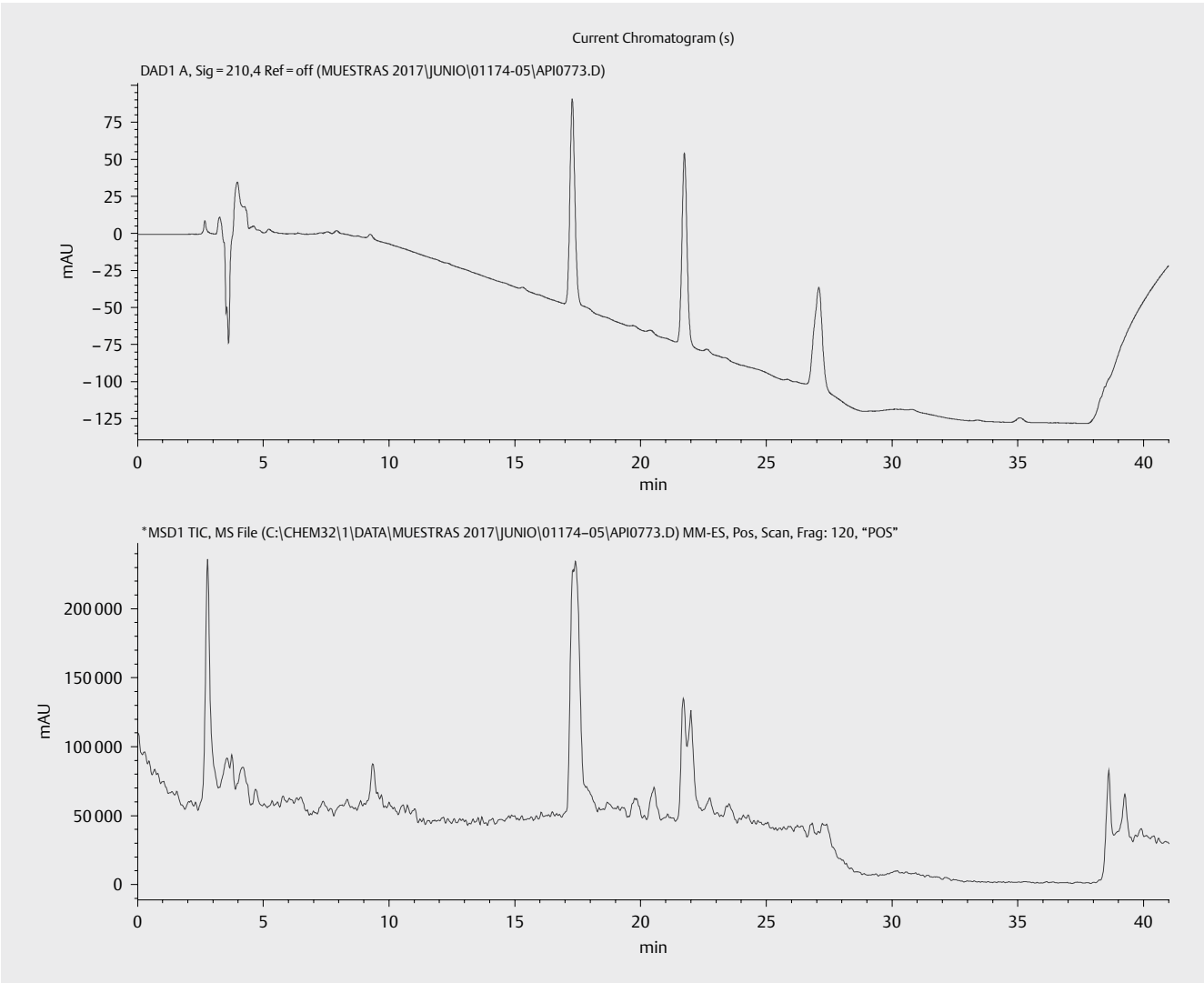
▶ **Fig. 2** Identification of macamides mixture in the HPLC chromatogram of sub-fraction IIID of *T. tuberosum*.

Apaza et al. Anti-inflammatory Potential of Macamides… Planta Med Int Open 2020; 7: e88–e99

e93

ing for the structural differences between these compounds. Compounds (**1**) and (**2**) are composed of an unsaturated fatty acid residue (linoleic and oleic), which differs only by the presence of one additional double bond of compound (**1**) with respect to compound (**2**). This structural difference in compound (**1**) would allow it to easily traverse the cell membrane and the mitochondrial membrane, thus justifying the difference in activity [38].

Likewise, the compounds (*N*-benzyllinoleamide and *N*-benzyloleamide) showed anti-inflammatory activity at 12 h of treatment in all the cell lines we analysed. With respect to the inhibition of TNF-α-induced NF-κB activation, compounds were compared with respect to the positive Celastrol control (IC$_{50}$ = 7.41 ± 0.99 μM). For this assay, Celastrol was chosen, a triterpene used to treat chronic inflammatory and autoimmune diseases. The concentration used in the trials was based on previous research [39].

Compound (**1**) showed increased activity on CCD-1109Sk (IC$_{50}$ = 2.28 ± 0.54 μM); MRC-5 (IC$_{50}$ = 3.66 ± 0.34 μM) and RWPE-1 (IC$_{50}$ = 4.48 ± 0.29 μM) cell lines with respect to compound (**2**) with IC$_{50}$ of 6.50 ± 0.75 μM (CCD-1109Sk); 7.74 ± 0.19 μM (MRC-5) and 8.37 ± 0.09 μM (RWPE-1), respectively. Additionally, compounds (**1**) and (**2**) also showed inhibition of TNF-α-induced NF-κB activation in control cells (THP-1) with IC$_{50}$ of 7.13 ± 0.02 μM and 9.78 ± 0.53 μM, respectively (▶ **Fig. 4**).
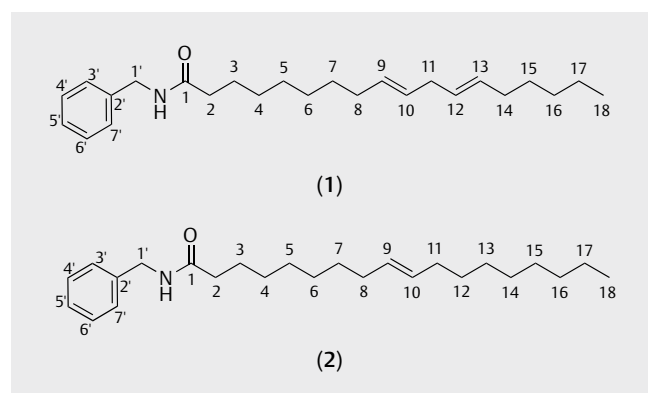
▶ **Fig. 3** Structures of compounds (**1**) and (**2**) of the yellow tubers from *T. tuberosum*.

NF-κB is one of the most important regulators of proinflammatory gene expression. We can indicate through our results that the inhibitory capacity of TNF-α-induced NF-κB activation by the macamides (*N*-benzyllinoleamide and *N*-benzyloleamide) is due to the direct inhibition of IκB kinase (IKK β) and to a lesser extent to the IKKα subunits of the κB inhibitor kinase complex (IκB) [24, 40]. Our results are comparable to the *N*-oleoyldopamine which was isolated from purple tubers of *T. tuberosum* [24]. This compound showed an inhibition of NF-κB by negative regulation, with an IC$_{50}$ of 3.54 ± 0.02 μM in THP-1 cells. However, *N*-benzyllinoleamide (**1**) and *N*-benzyloleamide (**2**) showed an IC$_{50}$ of 7.13 ± 0.02 μM and 9.78 ± 0.53 μM, respectively, in the same cell line. This significant difference can be attributed to the presence of the hydroxyl functional groups in the aromatic ring of the *N*-oleoyldopamine. Lastly, the mechanism described above for macamides is similar to the positive control (Celastrol) that blocks IKK activity, nuclear translocation and NF-κB activation [41].

Furthermore, we can indicate that the fatty acid residue (unsaturated fatty acid) present in *N*-benzyllinoleamide (**1**) and *N*-benzyloleamide (**2**) may be partly responsible for the activity in NF-κB. Indeed, PUFA-derived lipidic mediators, such as eicosanoids or endocannabinoids, can target transcription factors like NF-κB to modulate the gene expression involved in inflammatory disorders [42, 43].

Finally, our results show that the isolated compounds also inhibit the activation of STAT3 induced by IFN-γ, compared to the positive control AG 490 (IC$_{50}$ = 48 ± 0.80 μM). For this assay, compound AG 490 was chosen, an inhibitor of JAKs/STATs pathways with IC$_{50}$ value of 48 μM [44].

Compound (**1**) showed increased activity on CCD-1109Sk (IC$_{50}$ = 0.61 ± 0.76 μM); MRC-5 (IC$_{50}$ = 1.24 ± 0.05 μM) and RWPE-1 (IC$_{50}$ = 2.10 ± 0.12 μM) cell lines compared to compound **2** with IC$_{50}$ of 5.49 ± 0.31 μM (CCD-1109Sk); 7.73 ± 0.94 μM (MRC-5) and 7.79 ± 0.30 μM (RWPE-1), respectively. Additionally, compounds (**1**) and (**2**) also showed inhibition of the activation of STAT3 induced by IFN-γ in control cells (THP-1) with IC$_{50}$ of 6.78 ± 0.42 μM and 9.39 ± 0.11 μM, respectively (▶ **Fig. 5**).

Inhibition of STAT3 by means of different compounds can take place through different mechanisms such as: phosphorylation, dimerization, transcriptional activity, acting at sites such as JAKs, SH2, DBD [45]. Likewise, there are reports indicating that IFN-γ in-

▶ **Table 6** LDH and XTT assays of the compounds from *T. tuberosum* against a panel of human cell lines after 12 h of treatment.

Samples	% Viable cells			
	THP-1	**CCD-1109Sk**	**MRC-5**	**RWPE-1**
Untreated cells	99.95 ± 0.95	99.92 ± 0.87	98.96 ± 0.60	99.98 ± 0.75
Triton X-100	9.37 ± 0.28	9.18 ± 0.92	9.29 ± 0.74	10.44 ± 0.93
Compound **1**[a]	87.00 ± 0.07	80.59 ± 0.90	81.42 ± 0.12	82.79 ± 0.99
Compound **2**[a]	90.67 ± 0.58	90.62 ± 0.85	94.51 ± 0.07	95.33 ± 0.97
Untreated cells	98.95 ± 0.21	97.97 ± 0.72	99.91 ± 0.91	97.96 ± 0.86
Actinomycin D	47.30 ± 0.31	49.46 ± 0.88	48.61 ± 0.12	48.82 ± 0.27
Compound **1**[b]	89.96 ± 0.27	83.09 ± 0.53	85.09 ± 0.94	89.16 ± 0.57
Compound **2**[b]	92.45 ± 0.49	94.38 ± 0.11	98.45 ± 0.62	99.97 ± 0.39

[a]Cytotoxicity values of the LDH assay. [b]Viability values of the XTT assay. The results are the means (±SD) of three separate experiments performed in triplicate. Control = untreated cells. Significant difference among means (p < 0.0001)/Tukey's multiple comparisons test.
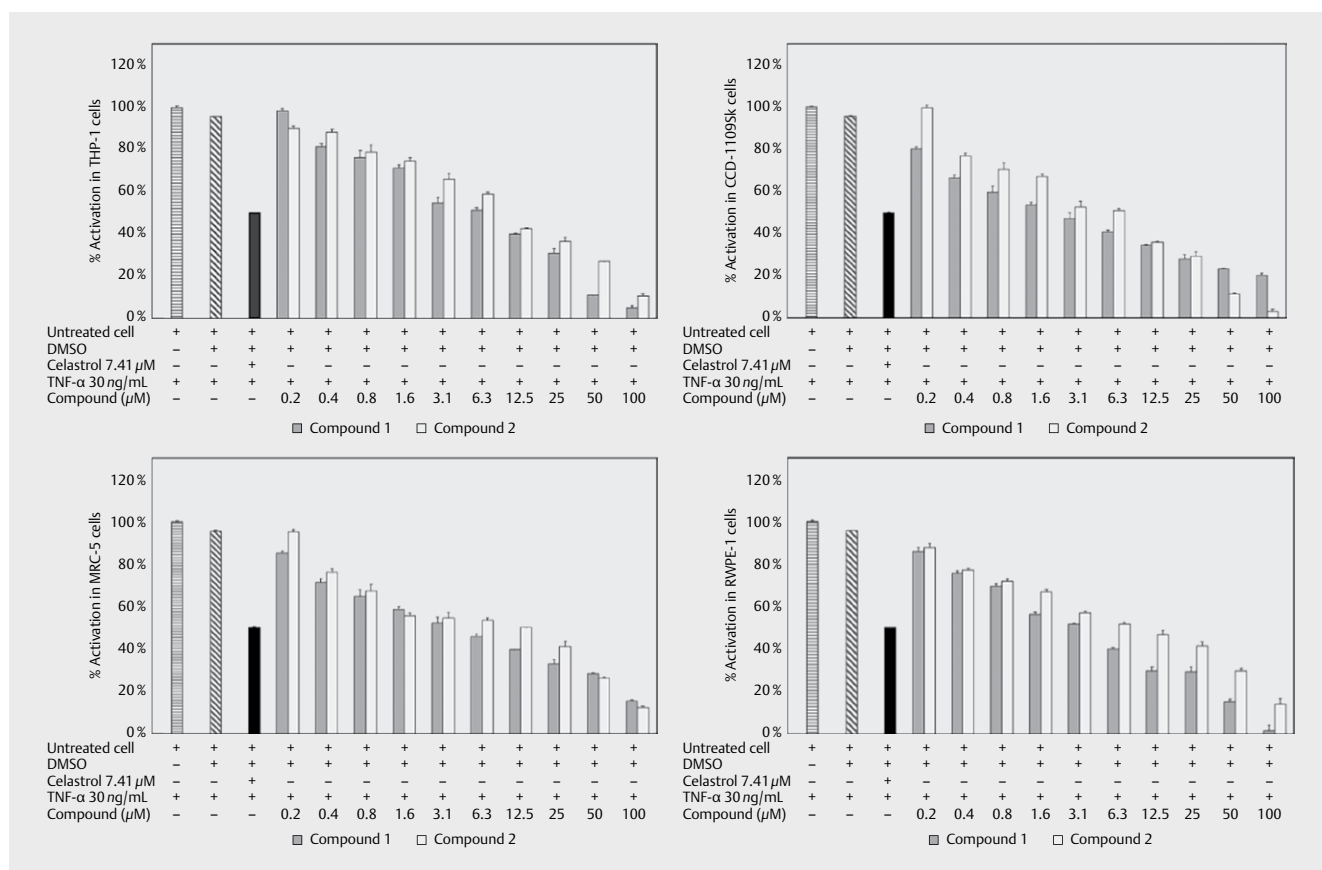
▶ **Fig. 4** Effect of the macamides on TNF-α-induced NF-κB activation. Results are represented as the percentage of inhibition considering 100 % the value of TNF-α-induced NF-κB activation. The results are the means (± SD) of three separate experiments performed in triplicate. Control (untreated cells). Significant diff. among means (P < 0.0001)/Tukey's multiple comparisons test.

duces the phosphorylation of STAT1, STAT3 and STAT5 through the JAK/STAT signalling pathway [46]. Through our experimental design, we determined that macamides can reduce STAT3 phosphorylation via JAK/STAT caused by IFN-γ stimulation, our research being the first report on the activity of macamides on STAT3. The mechanism of action of macamides can be comparable to that of the positive control (AG 490) that inhibits the JAK2, JAK3/STAT, JAK3/AP-1 and JAK3/MAPK pathways [44].

In this case, we can also indicate that the unsaturated fatty acid residue present in *N*-benzyllinoleamide (**1**) and *N*-benzyloleamide (**2**) may be partly responsible for the activity in STAT3. Mechanistic studies revealed that PUFAs show activity in certain inflammatory disorders that act on JAK-STAT3 signalling [47].

The activity assays of the *N*-benzylmiristamide and *N*-benzylpalmitamide macamides present in the sub-fraction IIID could not be determined because they were in a lower concentration with respect to the *N*-benzyllinoleamide (**1**) and *N*-benzyloleamide (**2**) macamides. However, if we analyse the fatty acid residue of these macamides we observe that they are saturated fatty acids. Previous studies indicate that unsaturated fatty acids (linoleic and oleic) have a higher anti-inflammatory activity compared to saturated fatty acids (myristic and palmitic) [48].

The importance of the isolation of this type of compounds is due to their chemical nature, since they can easily cross the intes-

tinal wall and the blood-brain barrier, exerting a greater pharmacological effect. Taking advantage of this property, there are studies that report the activity of macamides as FAAH inhibitors [49], as neuroprotectors *in vitro* and *in vivo* by means of a mechanism mediated by the CB1 receptor given that they present an analogous structure to endocannabinoidanandamide [50]. In this sense, *N*-benzyllinoleamide (**1**) and *N*-benzyloleamide (**2**) macamides may have potential therapeutic implications for inflammatory/autoimmune diseases mediated by NF-κB and STAT3.

In conclusion, this study has revealed the identification of four macamides (*N*-benzylmiristamide, *N*-benzylpalmitamide, *N*-benzyloleamide and *N*-benzyllinoleamide) for the first time in the yellow tubers of *T. tuberosum*. Furthermore, this work has corroborated that the consumption of cooked tubers of *T. tuberosum* can be a remedy for inflammatory processes of the skin, lungs and prostate.

Material and Methods

Plant material

The tubers of *T. tuberosum* were collected from Titicani-Taca which is located in Villa Asunción de Machaca canton of the Sixth Municipal Section Jesus de Machaca, in the Ingavi province of the La Paz

Apaza et al. Anti-inflammatory Potential of Macamides ... Planta Med Int Open 2020; 7: e88–e99

e95
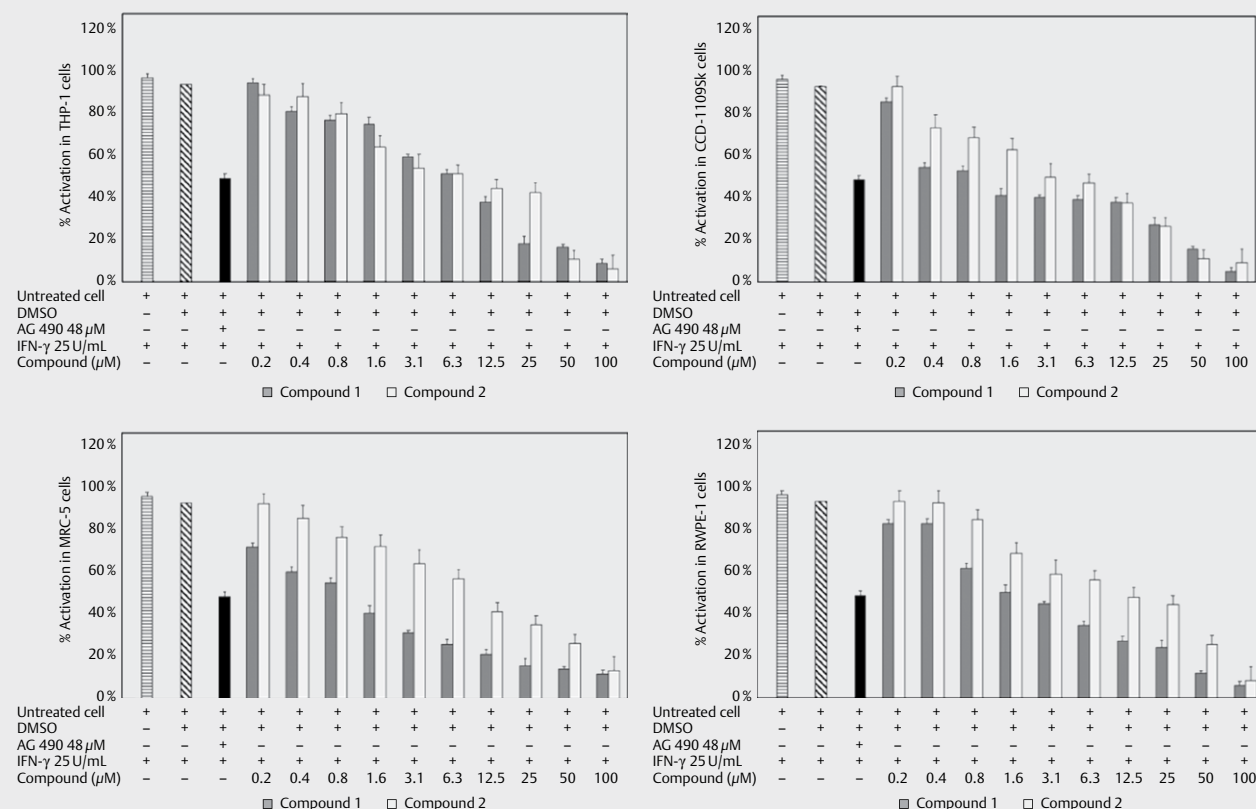
▶ **Fig. 5** Macamides inhibit IFN-γ-induced STAT3 activation. Results are represented as the percentage of inhibition considering 100 % the value of IFN-γ-induced STAT3 activation. The results are the means (±SD) of three separate experiments performed in triplicate. Control (untreated cells). Significant diff. among means (P<0.0001)/Tukey's multiple comparisons test.

department, Bolivia (16°44'24.5" S 68°48'49.2" W), in September 2015, at an altitude of 3900 m. Botanical identification was confirmed by the National Herbarium of Bolivia (No. 14898). Given the fact that yellow tubers are the most consumed Mashua ecotype [13], we have decided to work with this variety of *T. tuberosum* to confirm its potential as an anti-inflammatory.

General experimental design

All organic solvents used for isolation and purification were of ACS reagent grade and they were purchased from Sigma-Aldrich. TLC was performed using Merck silica gel 60-F_{254} plates. Chromatograms obtained were visualised by UV absorbance (254 nm) and through heating a plate stained with phosphomolybdic acid. Column chromatography was performed with 20–45 μm and 40–63 μm silica gel (Merck).

GC/MS analysis

The determination of FAMEs has been carried out on a Varian 3800 GC chromatograph, with a Varian 4000 MS ion trap detector. A flow of He of 1 mL/min and a HP-88 30 m x 0.25 mm (0.2 μm) were used. The injector temperature was 260 °C, the Split injection mode was 1/10 and the injection volume was 1 μL. The ionisation mode used was chemical ionisation, with the ionisation gas being MeOH.

In order to carry out the GC/MS analysis of the fatty acids, their methyl esters were prepared. 57.0 mg of the sample with 20 mL of a solution of HCl/MeOH (162.5 mL of 6 M HCl and 137.5 mL MeOH) were introduced into a flask [51]. The mixture was then heated at a temperature of 80 °C, at reflux, for half an hour. After this time, it was allowed to cool until the flask content reached room temperature. Subsequently, successive extractions of the aqueous phase were carried out, with 10 mL of a mixture of *n*-heptane/diethyl ether (1:1). Finally, the organic phase was washed with 10 mL of a 1 % NaOH solution, followed by a wash with 10 mL of distilled water. After drying the organic phase with anhydrous magnesium sulphate and subsequent filtration, it was concentrated by rota evaporation at a temperature of 40ºC and an initial pressure of 850 mbar and subsequently a pressure of 120 mbar to obtain 12 mg of a FAMEs mixture.

HPLC and LC/MS analysis

Macamides were analysed by the HPLC system (2695 pump, 2996 diode array detector; Agilent 1100 Series) coupled with an analytical column 200-C18–48 (4.6x250 mm), with a flow rate of 0.2 mL/ min. The detection wavelength that was used was 210 nm. The mobile phase used was composed of water and 0.1 % H-COOH (Phase A) and CH_3CN (Phase B). Elution was performed in gradient as fol-

e96

Apaza et al. Anti-inflammatory Potential of Macamides… Planta Med Int Open 2020; 7: e88–e99

lows: 0–24 min, 20–80 %; 24–30 min, 0–100 %; 30–31 min, 20–80 %; and 31–41 min, 20–80 %. The separation temperature was set at 30 °C.

Furthermore, a LC/MS experiment was performed using Agilent Technologies 6120 Quadrupole LC/MS mass detector (Agilent Technologies Inc., Santa Clara, CA, USA). Analytical identification was performed using MRM and ESI in positive mode. The operation conditions were as follows: capillary 2000 V, nebuliser 60 psi, 5 L/min dry gas flow rate at 250 °C. Agilent MassHunter Workstation was used for data acquisition and processing.

NMR and MS analysis

^{1}H-NMR spectra were recorded on 300 MHz Bruker Advance DRX instruments. ^{13}C-NMR spectra were recorded at 75 MHz on the same instruments. The deuterated solvents were $CDCl_3$-d_1; MeOD-d_4 and D_2O. Spectra were calibrated by assignment of the residual solvent peak to δ_H 7.26; δ_H 3.31 and δ_H 4.79 for $CDCl_3$, MeOD and D_2O, and δ_C 77.16 and δ_C 49.00, for $CDCl_3$ and MeOD. The complete assignment of protons and carbons was done by analysing the correlated ^{1}H-^{1}H-COSY, HSQC and HMBC spectra. Mass spectra were performed on a mass spectrometer with QTOF hybrid model QSTAR pulsar i analyser from the commercial company AB Sciex. The samples were analysed using the electrospray ionisation technique in positive ion detection mode. They were introduced into the mass spectrometer by direct infusion at a flow of 10 μL/min using a syringe pump.

Extraction and isolation

Dried yellow tubers of *T. tuberosum* (300 g) were repeatedly extracted at room temperature with *n*-heptane (7.16 g), CH_2Cl_2/MeOH (19.21 g) and distilled water (4.77 g). Each extract was evaluated for its anti-inflammatory effects in different cell lines, the *n*-heptane extract being more active. Therefore, the *n*-heptane extract was fractionated to identify the active compounds.

The bioactive extract of *n*-heptane (7 g) was fractionated with 200 g of silica gel (40–63 μm) on a column chromatography (2x50 cm), using a gradual gradient of *n*-heptane/AcOEt (20:1), obtaining 9 fractions (I–IX), where fraction III (502.2 mg) showed greater anti-inflammatory activity in all cell lines. Subsequently, fraction III was separated with 15 g of silica gel (40–63 μm) on a column chromatography (2x50 cm), using a gradual gradient of *n*-heptane/AcOEt (5:1), obtaining 6 sub-fractions (IIIA–IIIF) that showed anti-inflammatory activity in all cell lines tested, sub-fraction IIID (30.36 mg) being the most active. Sub-fraction IIID was then separated with 2.5 g of silica gel (20–45 μm) on a chromatography column (2 × 50 cm) with *n*-heptane/acetone (7:2) as eluent, obtaining 14 sub-fractions (IIID1–IIID14) with anti-inflammatory activity, the sub-fraction IIID2-compound (**1**) (1.2 mg) and IIID4-compound (**2**) (2.7 mg) being the most active.

Cell culture

Four human cell lines were used in this study: CCD-1109Sk (Human skin fibroblast, CRL-2361), MRC-5 (Human lung fibroblast, CCL-171), RWPE-1 (Human prostate epithelial, CRL-11609) and THP-1 (Human peripheral blood monocyte, TIB-202). All cell lines were obtained from the ATCC. Cells were cultured in specific media according to ATCC recommendations. The incubation condition for all cells was at an atmosphere of 95 % air and 5 % CO_2 at 37 °C.

DMEM (Sigma-Aldrich, St. Louis, MO, USA), FBS (Summit Biotechnology; Ft. Collins, CO) and PBS (SAFC Biosciences, Inc. Andover-Hampshire, UK) were used as culture mediums. L-glutamine was obtained from Applichem. Penicillin and streptomycin were purchased from Fisher Scientific (Pittsburgh, PA). For cytotoxicity and activity assays the compounds were dissolved in DMSO (Merck) at a concentration of 10 mM, while extracts and fractions were dissolved at 20 mg/mL in DMSO.

Cytotoxicity and viability assays

The cytotoxicity and cell viability of the samples was determined in a panel of three human cell lines (CCD-1109Sk, MRC-5 and RWPE-1) and a control cell line (THP-1) by means of the LDH and XTT assays at different concentrations (100, 50, 25, 12.5, 6.25, 3.125, 1563, 0.781, 0.391 and 0.95) in μg/mL (extracts and fractions) or μM (compounds).

LDH assay: The cells were seeded in 96-well plates at a density of 3x10^3 cells/well and incubated overnight at 37 °C in a humidified atmosphere of 5 % CO_2. Subsequently, the cells were treated with the extracts or compounds at different concentrations and using DMSO as a control for 12 h. Triton X-100 (Molecular Biology Grade Sigma-Aldrich, CAS Number 9002-93-1) was used as a positive control at a concentration of 16.51 mM, showing cell death. After 12 h of treatment with the extracts or compounds, 100 μL of culture supernatants were collected and incubated in the reaction mixture of the LDH kit (Innoprot Company). After 30 min, the reaction was stopped by the addition of 1 N HCl, and the absorbance at a wavelength of 490 nm was measured using a spectrophotometric ELISA plate reader (SpectraMax® i3, Molecular Devices).

XTT assay: The inhibition of H_2O_2-induced cytotoxicity by the extracts or compounds at various concentrations was tested by the method of XTT-formazan dye formation [52], using the abovementioned cell lines. These cells were sown (200 μL, 3 × 10^3 cells/well) in a 96-well plate and allowed to grow at 37 °C. After 12 h, medium was removed from all wells. 200 μL fresh medium was added to the control wells. Cells in each test well were treated with 0.1 mM H_2O_2 (prepared in medium) along with different concentrations of the extracts or compounds. Actinomycin D (≥ 95 % Sigma-Aldrich, CAS Number 50-76-0) was used as a positive control at a concentration of 7.97 nM, showing cell death. Cells in both control and test wells were re-incubated for 12 h maintaining the same conditions. After the treatment incubation period, medium in each well was substituted by 200 μL of fresh medium, followed by the addition of 50 μL of XTT (0.6 mg/mL) containing 25 μM PMS. The plate was further incubated for 4 h in the same conditions. Absorbance was measured at 450 nm (with a 630 nm reference filter) in a spectrophotometric ELISA plate reader (SpectraMax® i3, Molecular Devices, CA, USA).

NF-κB inhibition assay

All cells were stably transfected with the KBF-Luc plasmid, which contains three copies of NF-κB binding site (from major histocompatibility complex promoter), fused to a minimal simian virus 40 promoter driving the luciferase gene. Cells (3 × 10^3 for cells/well)

Apaza et al. Anti-inflammatory Potential of Macamides … Planta Med Int Open 2020; 7: e88–e99

e97

were seeded the day before the assay on 96-well plate. The cells were then treated with samples (extracts, fractions and compounds) at the same concentrations used in the viability tests for 15 min and then they were stimulated with 30 ng/mL TNF-α. Celastrol (≥ 98 % Sigma-Aldrich, CAS Number 34157-83-0) was used as a positive control at a concentration of 7.41 µM. After 12 h, the cells were washed twice with PBS and lysed in 50 µL lysis buffer containing 25 mM Tris-phosphate (pH 7.8), 8 mM MgCl$_2$, 1 mM DTT, 1 % Triton X-100 and 7 % glycerol, during 15 min at room temperature in a horizontal shaker. Luciferase activity was measured using a GloMax 96 microplate luminometer (Promega) following the instructions of the luciferase assay kit (Promega, Madison, WI, USA). The RLU was calculated and the results were expressed as percentage of inhibition of NF-κB activity induced by TNF-α (100 % activation). The experiments for each concentration of the test elements were performed in triplicate wells.

STAT3 inhibition assays

All cells were stably transfected with the 4xM67 pTATA TK-Luc plasmid. Cells (3×10^3 cells/well) were seeded on a 96-well plate the day before the assay. The cells were then treated for 15 min with samples (extracts, fractions and compounds) at the same concentrations used in the viability tests, and then stimulated with IFN-γ 25 IU/mL. AG 490 (≥ 99 % Sigma-Aldrich, CAS Number 133550-30-8) was used as a positive control at a concentration of 48 µM. After 12 h, the cells were washed twice with PBS and lysed in 50 µL lysis buffer containing 25 mM Tris-phosphate (pH 7.8), 8 mM MgCl$_2$, 1 mM DTT, 1 % Triton X-100 and 7 % glycerol, during 15 min at room temperature in a horizontal shaker. Luciferase activity was measured using the GloMax 96 microplate luminometer (Promega) following the instructions of the luciferase assay kit (Promega, Madison, WI, USA). The RLU was calculated and the results were expressed as percentage of inhibition of STAT3 activity induced by IFN-γ (100 % activation). The experiments for each concentration of the test elements were performed in triplicate wells.

Statistical analysis

The statistical significance of differences was calculated employing the GraphPad Prism software, version 8.2.1 (GraphPad Software Inc., San Diego, CA, USA), using one-way ANOVA followed by Tukey's post hoc test for multiple comparisons. Results were considered different when $p < 0.0001$. IC$_{50}$ values were determined by non-linear regression using GraphPad Prism, version 8.2.1. All the experiments were performed in triplicate.

Supporting Information

Supplementary data (NMR and MS data of compounds) associated with this article can be found in the online version.

Author Contribution

ARS and MRC contributed to the analysis of the spectral data; LAT and GP contributed to the conception and experimental design of the pharmacological study and LAT contributed to the writing and review of the manuscript.

Conflict of Interest

The authors declare that they have no conflict of interest.

References

[1] Hunter P. The inflammation theory of disease. EMBO Rep 2012; 13: 968–970

[2] Krishnamoorthy S, Honn KV. Inflammation and disease progression. Cancer Metastasis Rev 2006; 25: 481–491

[3] Rumel C. Inflammatory transcription factors as activation markers and functional readouts in immune-to-brain communication. Brain Behav Immun 2016; 54: 1–14

[4] Vallabhapurapu S, Karin M. Regulation and function of NF-kappaB transcription factors in the immune system. Annu Rev Immunol 2009; 27: 693–733

[5] Hayden MS, Ghosh S. Shared principles in NF-kappaB signaling. Cell 2008; 132: 344–362

[6] Levy DE, Lee CK. What does Stat3 do? J Clin Invest 2002; 109: 1143–1148

[7] Herrmann A, Vogt M, Mönnigmann M, Clahsen T, Sommer U, Haan S, Poli V, Heinrich PC, Müller-Newen G. Nucleocytoplasmic shuttling of persistently activated STAT3. J Cell Sci 2007; 120: 3249–3261

[8] Yu H, Pardoll D, Jove R. STATs in cancer inflammation and immunity: A leading role for STAT3. Nat Rev Cancer 2009; 9: 798–809

[9] Yang J, Liao X, Agarwal MK, Barnes L, Auron PE, Stark GR. Unphosphorylated STAT3 accumulates in response to IL-6 and activates transcription by binding to NFkappaB. Genes Dev 2007; 21: 1396–1408

[10] Fan Y, Mao R, Yang J. NF-κB and STAT3 signaling pathways collaboratively link inflammation to cancer. Protein Cell 2013; 4: 176–185

[11] Bent S. Herbal Medicine in the United States: Review of efficacy, safety, and regulation. J Gen Intern Med 2008; 23: 854–859

[12] Tasneem S, Liu B, Li B, Choudhary MI, Wang W. Molecular pharmacology of inflammation: Medicinal plants as anti-inflammatory agents. Pharmacol Res 2019; 139: 126–140

[13] Apaza TL, Tena VP, Bermejo PB. Local/traditional uses, secondary metabolites and biological activities of Mashua (Tropaeolum tuberosum Ruíz & Pavón). J Ethnopharmacol 2020; 247: 112152

[14] Fernández HAM, Rodríguez REF. Etnobotánica del Peru Pre-Hispano. 1st Edition. Trujillo: Ediciones Herbarium Truxillense (HUT); 2007: 133–134

[15] De Lucca DM, Zalles AJ. Flora Medicinal Boliviana. 1st Edition. Cochabamba: Los Amigos del Libro; 1992: 401

[16] De Lucca DM, Zalles AJ. Utasan Utjir Qollanaka. Medicinas junto a nuestra casa. 1st Edition. La Paz: Agencia Española de Cooperación Internacional; 2006: 88

[17] Espinosa P, Abad J, Vaca R. Diagnostico de las limitantes de producción y consumo de las raíces y tubérculos andinos en Ecuador. 1st Edition. Ecuador: Instituto Nacional de Investigaciones Agropecuarias (INIAP); 1994 pp. irr

[18] Monteros Altamirano AR. Estudio de la Variación Morfológica e Isoenzimatica de 78 entradas de Mashua (Tropaeolum tuberosum R & P.). "Santa Catalina"-INIAP [dissertation]. Ecuador: Universidad Central de Ecuador; 1996

e98

Apaza et al. Anti-inflammatory Potential of Macamides … Planta Med Int Open 2020; 7: e88–e99

[19] Chirinos R, Campos D, Costa N, Arbizu C, Pedreschi R, Larondelle Y. Phenolic profiles of Andean mashua (Tropaeolum tuberosum Ruiz & Pavón) tubers: Identification by HPLC-DAD and evaluation of their antioxidant activity. Food Chem 2008; 106: 1285–1298

[20] Chirinos R, Campos D, Arbizu C, Rogez H, Rees JF, Larondelle Y, Noratto G, Cisneros-Zevallos L. Effect of genotype, maturity stage and post-harvest storage on phenolic compounds, carotenoid content and antioxidant capacity, of Andean mashua tubers (Tropaeolum tuberosum Ruiz & Pavón). J Sci Food Agric 2007; 87: 473–446.

[21] Chirinos R, Campos D, Betalleluz I, Giusti MM, Schartz SJ, Tian Q, Pedreschi R, Larondelle Y. High performance liquid chromatography with photodiode array detection (HPLC/DAD)/HPLC-Mass spectrometry (MS) profiling of anthocyanins from Andean Mashua tubers (Tropaeolum tuberosum Ruíz & Pavón) and their contribution to the overall antioxidant activity. J Agr Food Chem 2006; 54: 7089–7097

[22] Martín JC, Ligia HB. Glucosinolate composition of Colombian accessions of Mashua (Tropaeolum tuberosum Ruíz & Pavón), structural elucidation of the predominant glucosinolate and assessment of its antifungal activity. J Sci Food Agric 2016; 96: 4702–4712

[23] Ramallo RZ. Análisis exploratorio de los ácidos grasos del Isaño (Tropaeolum tuberosum). Investigación & Desarrollo 2004; 4: 69–74

[24] Apaza TL, Tena VP, Serban AM, Alonso NMJ, Rumbero A. Alkamides from Tropaeolum tuberosum inhibit inflammatory response induced by TNF-α and NF-κB. J Ethnopharmacol 2019; 235: 199–205

[25] White J. Notes on the Biology of Oxalis tuberosa and Tropaeolum tuberosum. Thesis in Biology. Harvard College 1975; 96

[26] Terrazas F, Valdivia F. Spatial dynamics of in situ conservation: handling the genetic diversity of Andean tubers in mosaic systems. Plant Genet Resour Newsl 1998; 114: 9–15

[27] Johns T, Kitts WD, Newsome F, Towers GHN. Anti-reproductive and other medicinal effects of Tropaeolum tuberosum. J Ethnopharmacol 1982; 5: 149–161

[28] García H. Flora medicinal de Colombia. Botánica Médica. Instituto de Ciencias Naturales. Universidad Nacional; Bogotá: 1975; 15–18

[29] Herrera FL. Contribución a la flora del departamento del Cuzco. Perú; Primera parte. Universidad del Cuzco; Cuzco, Perú: 1921

[30] Chan FKM, Moriwaki K, De Rosa MJ. Detection of Necrosis by Release of Lactate Dehydrogenase (LDH) Activity. Methods Mol Biol 2013; 979: 65–70

[31] Roehm NW, Rodgers GH, Hatfield SM, Glasebrook AL. An improved colorimetric assay for cell proliferation and viability utilizing the tetrazolium salt XTT. J Immunol Methods 1991; 142: 257–265

[32] de Sousa Andrade IP, Folegatti MV, Almeida Santos ON, Fanaya Junior ED, Barison A, da Conceição Santos AD. Fatty acid composition of Jatropha curcas seeds under different agronomical conditions by means of 1H HR-MAS NMR. Biomass Bioenerg 2017; 101: 30–34

[33] Liu H, Jin W, Fu C, Dai P, Yu Y, Huo Q, Yu L. Discovering anti-osteoporosis constituents of maca (Lepidium meyenii) by combined virtual screening and activity verification. Food Res Int 2015; 77: 215–220

[34] Huang YJ, Peng XR, Qiu MH. Progress on the chemical constituents derived from glucosinolates in maca (Lepidium meyenii). Nat Prod Bioprospect 2018; 8: 405–412

[35] Chen JJ, Gong PF, Liu YL, Liu BY, Eggert D, Guo YH, Zhao MX, Zhao QS, Zhao B. Postharvest ultrasound-assisted freeze-thaw pre-treatment improves the drying efficiency, physicochemical properties, and macamide biosynthesis of maca (Lepidium meyenii). J Food Sci 2018; 83: 966–974

[36] Arnott JA, Planey SL. The influence of lipophilicity in drug discovery and design. Expert Opin Drug Discov 2012; 7: 863–875

[37] Vetten MA, Tlotleng N, Rascher DT, Skepu A, Keter FK, Boodhia K, Koekmoer LA, Andreaos C, Tshikhudo R, Gulumian M. Label-free in vitro toxity and uptake assessment of citrate stabilised gold nanoparticles in three cell lines. Part Fibre Toxicol 2013; 10: 1–15.

[38] Hawkins RA, Sangster K, Arends MJ. Apoptotic death of pancreatic cancer cells induced by polyunsaturated fatty acids varies with double bond number and involves an oxidative mechanism. J Pathol 1998; 185: 61–70

[39] Nagase M, Oto J, Sugiyama S, Yube K, Takaishi Y, Sakato N. Apoptosis induction in HL-60 cells and inhibition of topoisomerase II by triterpene celastrol. Biosci Biotechnol Biochem 2003; 67: 1883–1887

[40] Sancho R, Calzado MA, Di Marzo V, Appendino G, Muñoz E. Anandamide inhibits nuclear factor-κB activation through a cannabinoid receptor-independent pathway. Mol Pharmacol 2003; 63: 429–438

[41] Simmonds RE, Foxwell BM. Signalling, inflammation and arthritis: NF-kappaB and its relevance to arthritis and inflammation. Rheumatology 2008; 47: 584–590

[42] Ibrahim A, Mbodji K, Hassan A, Aziz M, Boukhettala N, Coëffier M, Savoye G, Déchelotte P, Marion-Letellier R. Anti-inflammatory and anti-angiogenic effect of long chain n-3 polyunsaturated fatty acids in intestinal microvascular endothelium. Clin Nutr 2011; 30: 678–687

[43] Marion-Letellier R, Savoye G, Ghosh S. Polyunsaturated fatty acids and inflammation. IUBMB Life 2015; 67: 659–667

[44] Mielecki M, Lesyng B. Cinnamic acid derivatives as inhibitors of oncogenic protein kinases-structure, mechanisms and biomedical effects. Curr Med Chem 2016; 23: 954–982

[45] Chen Q, Lv J, Yang W, Xu B, Wang Z, Yu Z, Wu J, Yang Y, Han Y. Targeted inhibition of STAT3 as a potential treatment strategy for atherosclerosis. Theranostics 2019; 9: 6424–6442

[46] Fang P, Hwa V, Rosenfeld RG. Interferon-gamma-induced dephosphorylation of STAT3 and apoptosis are dependent on the mTOR pathway. Exp Cell Res 2006; 312: 1229–1239

[47] Yan D, Yang Q, Shi M, Zhong L, Wu C, Meng T, Yin H, Zhou J. Polyunsaturated fatty acids promote the expansion of myeloid-derived suppressor cells by activating the JAK/STAT3 pathway. Eur J Immunol 2013; 43: 2943–2955

[48] Calder PC, Grimble RF. Polyunsaturated fatty acids, inflammation and immunity. Eur J Clin Nutr 2002; 56: S14–S19

[49] Wu H, Kelley CJ, Pino-Figueroa A, Vu HD, Maher TJ. Macamides and their synthetic analogues: Evaluation of in vitro FAAH inhibition. Bioorg Med Chem 2013; 21: 5188–5197

[50] Gugnani KS, Vu N, Rondón-Ortiz AN, Böhlke M, Maher TJ, Pino-Figueroa AJ. Neuroprotective activity of macamides on manganese-induced mitochondrial disruption in U-87 MG glioblastoma cells. Toxicol Appl Pharmacol 2018; 340: 67–76

[51] Yang C, Guo ZB, Du ZM, Yang HY, Bi YJ, Wang GQ, Tan YF. Cellular fatty acids as chemical markers for differentiation of Acinetobacter baumannii and Acinetobacter calcoaceticus. BES 2012; 56: 5–51

[52] Weislow OS, Kiser R, Fine DL, Bader J, Shoemaker RH, Boyd MR. New soluble-formazan assay for HIV-1 cytopathic effects: application to high-flux screening of synthetic and natural products for AIDS-antiviral activity. JNCI 1989; 81: 577–586

Apaza et al. Anti-inflammatory Potential of Macamides… Planta Med Int Open 2020; 7: e88–e99

e99